

Uplink Array Concept Demonstration with the EPOXI Spacecraft

V. Vilnrotter, D. Lee, T. Cornish, P. Tsao, L. Paal, V. Jamnejad
Jet Propulsion Laboratory
4800 Oak Grove Dr.
Pasadena, CA 91109
(818) 354-2745
Victor.A.Vilnrotter@jpl.nasa.gov

Abstract — Uplink array technology is currently being developed for NASA's Deep Space Network (DSN), to provide greater range and data throughput for future NASA missions, including manned missions to Mars and exploratory missions to the outer planets, the Kuiper belt, and beyond. The DSN uplink arrays employ N microwave antennas transmitting at X-band to produce signals that add coherently at the spacecraft, thereby providing a power gain of N^2 over a single antenna. This gain can be traded off directly for N^2 higher data rate at a given distance such as Mars, providing for example HD quality video broadcast from earth to a future manned mission, or it can provide a given data-rate for commands and software uploads at a distance N times greater than would be possible with a single antenna. The uplink arraying concept has been recently demonstrated using the three operational 34-meter antennas of the Apollo complex at Goldstone, CA, which transmitted arrayed signals to the EPOXI spacecraft. Both two-element and three-element uplink arrays were configured, and the theoretical array gains of 6 dB and 9.5 dB, respectively, were demonstrated experimentally. This required initial phasing of the array elements, the generation of accurate frequency predicts to maintain phase from each antenna despite relative velocity components due to earth-rotation and spacecraft trajectory, and monitoring of the ground system phase for possible drifts caused by thermal effects over the 16 km fiber-optic signal distribution network. This paper provides a description of the equipment and techniques used to demonstrate the uplink arraying concept in a relevant operational environment. Data collected from the EPOXI spacecraft is also analyzed to verify array calibration, array gain, and system stability over the entire 5 hour duration of this experiment.

TABLE OF CONTENTS

1. INTRODUCTION.....	1
2. UPLINK ARRAYING CONCEPT.....	1
3. GROUND SYSTEM MONITORING AND CONTROL.....	3
4. UPLINK ARRAY EXPERIMENT RESULTS.....	4
5. SUMMARY AND CONCLUSIONS.....	6
REFERENCES	7
BIOGRAPHY	7

1. INTRODUCTION

Coherent arraying of antennas transmitting uplink signals to a spacecraft is a novel concept that will greatly increase NASA's deep-space communications capabilities in the future. Typically, deep-space missions require the capability to command the spacecraft right after launch, during cruise, and after encountering the target, in order to provide two-way communication and ranging. In addition, in-flight reconfiguration may be required to accommodate unforeseen changes in mission objectives. The use of antenna arrays enables much greater data-rates, greater effective operating distance, and cost-effective scaling for more demanding future missions through a highly flexible design philosophy, via the inherently parallel architecture of antenna arrays.

On June 27th 2008, NASA's Deep Space Network configured an array of three 34 meter antennas located at the Apollo station to transmit coherently combined signals to the EPOXI spacecraft, yielding nine times greater signal power than previously possible with a single antenna. Prior to this experiment, only single 34-meter or 70-meter antennas had been used to transmit uplink signals. Successful coherent arraying of three DSN antennas is a major step towards demonstrating future uplink array capabilities, greatly extending the DSN's reach into deep space.

During this experiment X-band signals were combined from three 34-meter antennas at the Goldstone complex near the Mojave Desert, and transmitted to the EPOXI. The EPOXI spacecraft received the combined signals, measured the combined power levels, and verified the predicted array power gains of 6 dB and 9.5 dB over a single antenna, for both two- and three-antenna arrays. In addition, non-operational (or No-Op) test-messages that resemble real uplink commands (but are ignored by the spacecraft) were transmitted, all of which were received and acknowledged..

2. UPLINK ARRAYING CONCEPT

The primary goal of this experiment was to illuminate the EPOXI spacecraft simultaneously with two and three X-band carriers, using the 34-m BWG antennas at the Goldstone Apollo complex (DSS-24, DSS-25 and DSS-26), to determine the stability of the arrayed carrier power at the

spacecraft, and transmit realistic No-Op commands to the spacecraft at the maximum possible rate. The actual physical configuration of the Apollo complex antennas is shown in Fig 1, where DSS-26 is nearest, and DSS-24 farthest along a north-northwest baseline.



Figure 1. The Apollo complex of 34m BWG antennas at the Goldstone Deep Space Complex.

A conceptual diagram of the experimental setup is shown in Fig. 2, similar to the previous experiment carried out earlier with the Mars Global Surveyor spacecraft, and reported in [1]. The central antenna (DSS-25) was designated as the reference antenna during this experiment, and was the only antenna configured to receive EPOXI downlink telemetry and transmit X-band uplink. The telemetry contained 5 second updates of the Small Deep-Space Transponder (SDST) wide-band AGC reading (WB AGC), narrow-band AGC readings (NBAGC), as well as 5 second updates of the coherent lock accumulator (CLA) which provided the most accurate estimate of received carrier power. The other two antennas were employed in transmit mode only.

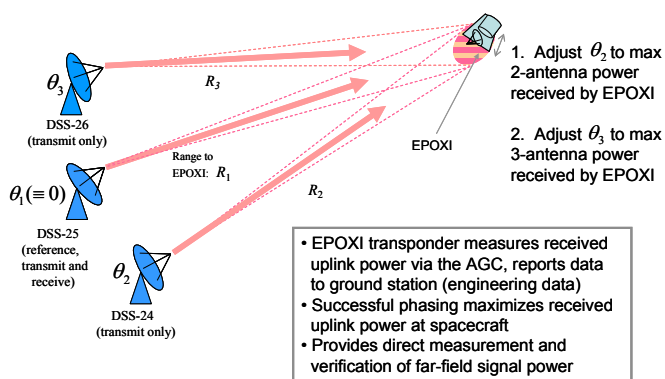


Figure 2. EPOXI Uplink Array Experiment conceptual block diagram

Differential Doppler caused by earth-rotation was removed using extremely accurate frequency predicts developed especially for uplink array applications, and applied to the exciters at SPC-10 prior to transmission. Examples of the steady-state Doppler-compensated two- and three-antenna

power distributions in the vicinity of the spacecraft are shown in the simulated far-field patterns of Figs. 4a-d. The actual antenna positions at the Apollo complex were used to calculate these patterns, for a target located at zenith. In all cases, the arrayed power distribution in the far-field is the product of the primary antenna pattern and the interference pattern generated by two or three point-sources located at the antenna phase-centers.

It can be seen from Figs. 3 that arrays composed of a few 34m antennas have a considerable advantage in emergency communications over irregularly spaced “large arrays” of small antennas, since the regular structure of the far-field array pattern can be used to greatly reduce the time it takes to locate a lost probe. These patterns were calculated at the distance of the Moon, and previously used to explain the effects of array illumination on a selected lunar target [2]. For the two-antenna arrays, a very efficient “array-search” can be performed simply by adding 180 degrees to the phase of one of the antennas, thus exchanging the location of the array peaks and array nulls within the entire single-antenna beam: therefore, the entire 34m single-antenna beamwidth can be covered with a single operation.

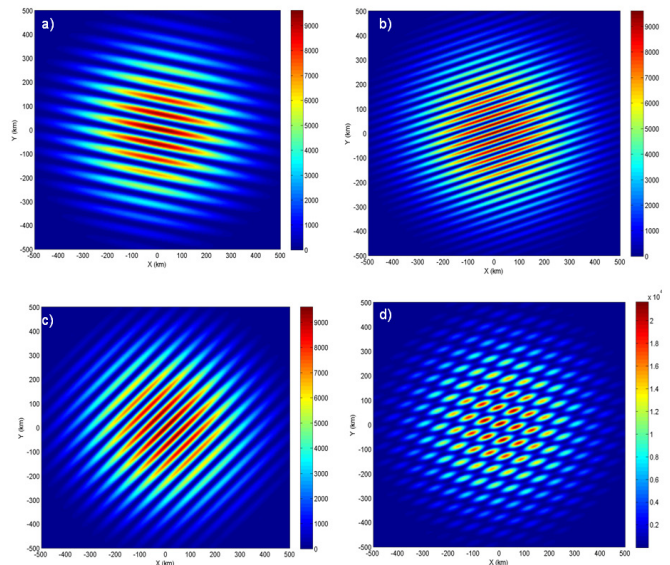


Figure 3. Far field power distributions generated by two and three element arrays of the Apollo complex.

Pointing of the two antennas toward the spacecraft to a small fraction of the primary beamwidth is routinely achieved with the operational antennas of the Apollo complex. However, this does not guarantee that the peak of the interference pattern generated by two- and three-antenna arrays illuminating the spacecraft will be maximized: the transmitted phases have to be aligned at the spacecraft in order to achieve maximized combined power. Initially, the spacecraft may be located near the peak or the null of the two-antenna interference pattern, but most likely at some intermediate point on the array gain profile. Examples of simulated far-field power distributions generated by two and three antenna array configurations perpendicular to the

baseline, are shown in Fig. 3. Note that peaks and nulls occur closely spaced in the interference pattern, with fringe distance inversely proportional to the length of the baseline for the two-antenna configurations, requiring precise electronic beam-steering to point the peak of the array pattern towards EPOXI.

During the experiment, the EPOXI high gain antenna (HGA) was pointed towards earth: this meant that transmitter power levels of only 2 kw had to be used with all three antennas, in order not to saturate the CLA readings (even though the transmitters could deliver a maximum of 20 kw). At the beginning of the track, the DSS-25 transmitter was commanded to transmit a 2kw X-band carrier, and executed an operational uplink frequency sweep to ensure that the small deep-space transponder (SDST) aboard EPOXI acquired the signal one light-time later (OWLT=172 secs). One round-trip light-time later (RTLT=344 secs), the DSS-25 ground station receiver acquired and locked onto the downlink carrier, and began recording engineering telemetry from the spacecraft. The engineering telemetry contained readouts from the WBAGC, NBAGC and CLA, providing updates of the received uplink carrier power once every five seconds.

3. GROUND SYSTEM MONITORING AND CONTROL

Slowly varying phase drifts in the ground system are monitored and controlled by the Phase Comparator and Control Assembly (PCCA), located in a half-rack at SPC-10. The PCCA contains a signal distribution assembly (SDA), two phase comparator assemblies (PCA) to measure round-trip and cross phase from all three Apollo antennas, and a phase modulation assembly (PMA) that can be used to add correction phases to either the DSS-24 or the DSS-26 carriers.

The theory of operation for the PCCA has been fully described in a previous article [3]. In summary, the ground system consists of the X-band exciters at SPC-10, X-band couplers, and a “round-trip” phase comparator assembly at SPC-10, optical fibers for signal distribution to the transmitting antennas, X-band couplers at the output of the power amplifiers at each antenna, and additional optical fibers to return the coupled signal samples to SPC-10 for comparison. The two-way optical fiber distribution network to and from the antennas is located in the same bundle for most of the 16 km distance from SPC-10 to the Apollo cluster, ensuring similar thermal behavior for the outgoing and returning signals. At the Apollo station the individual fibers are broken out from the common bundle and routed to their respective antennas, typically a distance of a few hundred meters, over which the fibers may experience slightly different thermal environments.

A small fraction of the amplified X-band signal is coupled at the output of the transmitter power amplifier (PA) and

routed back to SPC-10, where the phase of the signal is compared to that of the transmitted phase, using the real-time PCA. The inputs to the PCA are the outgoing and return signals from all three array antennas (DSS-24, DSS-25 and DSS-26 at the Apollo Complex). The PCA outputs consist of complex samples of equal magnitude representing the phase differences between the reference and return signals.

The phase errors introduced in the PCA by RF mixer phase imbalance and amplifier biases were processed using a Labview interface. The PCA is designed to provide roughly 5 degrees rms accuracy after calibration. The phase measurement accuracy was estimated based on analysis of component VSWR and phase imbalance. The power levels of the DSS-24 and DSS-25 reference and sample signals were measured using transmitter settings of 2 kw, which is the lowest practical power level that can be used without risk of transmitter instabilities. A 100 Hz low pass filter is applied at baseband after the RF mixers to reduce noise and smooth out fluctuations. After amplification, the baseband signals are sampled by an 8-channel 16-bit analog-to-digital converter. These samples are processed in Labview to remove any DC offsets and gain differences between the I and Q channels, and the appropriate phases computed as the 4-quadrant arctangent of the I and Q baseband signals.

The host computer of the PCCA was used to measure the round-trip and cross phases between two baselines, namely the DSS-24/25 and the DSS-25/26 baselines. Baseband I and Q samples were taken 100 times a second, and averaged to obtain 1-second estimates from which the phases were computed. A complete record of the cross-phase behavior of the DSS-24/25 baseline for the entire track is shown in Fig. 4a, for all three predict-sets. Note that the cross-phase jumps to different random values each time a new predict-set is loaded, since the exciters are not designed to maintain constant phase between predict-sets. However, the cross-phase remains essentially constant throughout each predict-set, indicating long-term stability on the order of a few degrees. Fig. 4b represents the difference of the round-trip phase measured for the same baseline: note that the round-trip phase is not subject to phase-jumps when a new predict-set is loaded in, since the return sample carrier is compared to the transmitted reference carrier for the same channel, hence a change in transmitted carrier phase is not registered by the PCA: only changes in phase applied after the reference coupler are registered, whether they are due to an applied phase offset via the PMA, or to unintended change in electrical pathlength due to thermal effects. It can be seen that the round-trip phase remained stable throughout the track, hence phase corrections did not have to be applied to compensate for ground-phase drift. Similar behavior was exhibited by the DSS-25/26 baseline during this track.

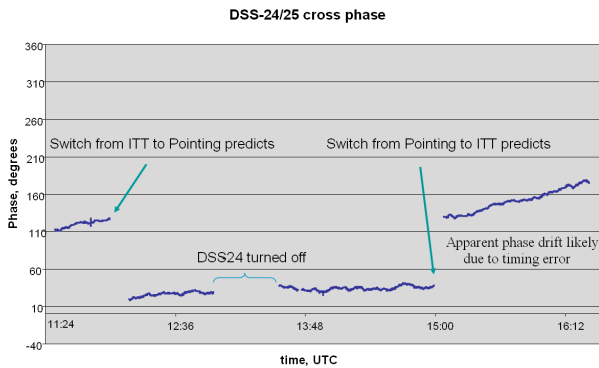


Figure 4a. DSS-24/25 cross-phase history covering the entire track

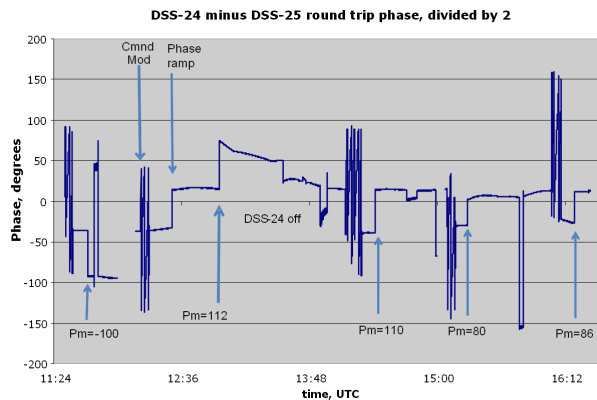


Figure 4b. Round-trip phase history, DSS-24 phase minus DSS-25 phase, divided by two

4. UPLINK ARRAY EXPERIMENT RESULTS

The EPOXI track started at 11:00:00 UTC, when the spacecraft was at an elevation of approximately 30 degrees, rising. Operationally supplied frequency predicts were used for the first predict interval. These predicts were not corrected for tropospheric variations, however differential phase build-up due to the troposphere was found to be insignificant above 30 degrees elevation, leading at most to 20 degrees over the DSS-24/25 baseline. The DSS-25 transmitter was configured for 2 kilowatts (kw) uplink power, with right-hand circular polarization (RCP). Transmission started shortly after 11:00 UTC on DOY-179 (June 27th), with a predetermined operational frequency ramp sequence to ensure carrier capture by the SDST phase-lock loop. The one-way light-time during this experiment was approximately 172 seconds, or 2 minutes 52 seconds, hence the first power estimate from the spacecraft was observed nearly 6 minutes after transmission. Data was recorded with the wide-band AGC (WBAGC), narrow-band AGC (NBAGC), and the carrier lock accumulator (CLA). As shown in Figure 5a, CLA records were received shortly after 11:00 on the spacecraft, one light-time after transmission started. In these and subsequent figures, the time axis refers to spacecraft time in UTC, not ground time. Note that the SDST locked onto the DSS-25 signal at roughly -103 dBm of carrier power, close to the predicted

value. This power level was well within the linear region of the WBAGC, whose resolution is 1.5 dB, but near the saturation region of the CLA, hence the initial readings appear lower than the true power measured by the spacecraft.

Corrections were applied to the digital numbers (DN) returned by the CLA during post-processing, via temperature dependent distortion profiles. Calibration curves for 25C and 60C baseplate temperatures were available from previous calibration, however the true baseplate temperature during this experiment was approximately 42.5 degrees, hence the corrections had to be interpolated to this temperature. The corrected values were used to generate Figs 5a-d, all of which are referenced to spacecraft time, termed “spacecraft event time” or SCET.

After the SDST locked up to the DSS-25 carrier, 16 KHz uplink modulation was turned on, and a sequence of ten No-Op commands sent to the spacecraft at about 11:12 SCET, recorded as a drop in CLA power from -102.7 dBm to -113 dBm in Fig. 12a. Since the CLA measures the carrier power, the power in the sidebands is lost to the CLA. However, since the mod index was 0.94 rads, only 5.8 dB should have been lost to modulation, not the approximately 10 dB drop shown in Fig. 12a. One reason for the discrepancy is that the correction curve is different for the modulated carrier, but this correction curve was only available for 25C, hence could not be interpolated to different baseplate temperatures.

Following successful reception and acknowledgement of all ten of the first set of No-Op commands by EPOXI at about 11:13 SCET, the modulation on the DSS-25 carrier was turned off, the DSS-24 transmitter drive was turned on, and the sum of the two carriers received by EPOXI at 11:18 SCET, as shown in Fig. 5a. The AGC readings were updated every 5 seconds, with a resolution of 0.3 dB on the CLA.

The far-field intensity produced by the two-antenna uplink array can be steered over the spacecraft electronically from the ground by varying one of the transmitter phases. When the differential phase varies over the entire range of $(0, 2\pi)$ radians, it is guaranteed that the peak of the intensity pattern illuminates the spacecraft, provided the phases are stable over the duration of the sweep. This power variation were measured by the spacecraft AGC to monitor the instantaneous carrier power at the spacecraft. The results of these measurements were then relayed to the ground as engineering data, and evaluated to determine the optimal phase adjustment required to phase up the signals at the spacecraft.

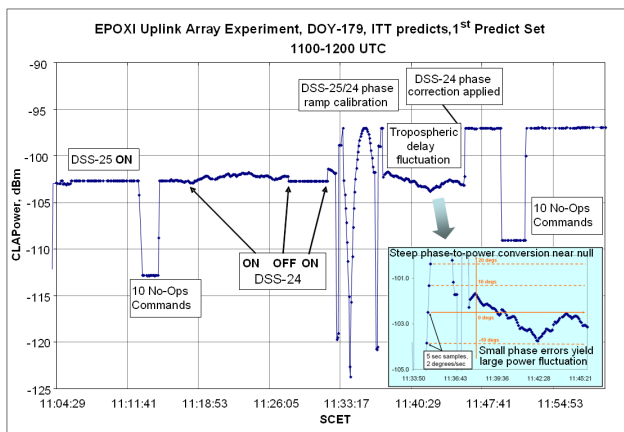


Figure 5a. Real-time CLA data at the start of the experiment, including examples of No-Op commands and phase-ramp sequence for estimating optimum phase.

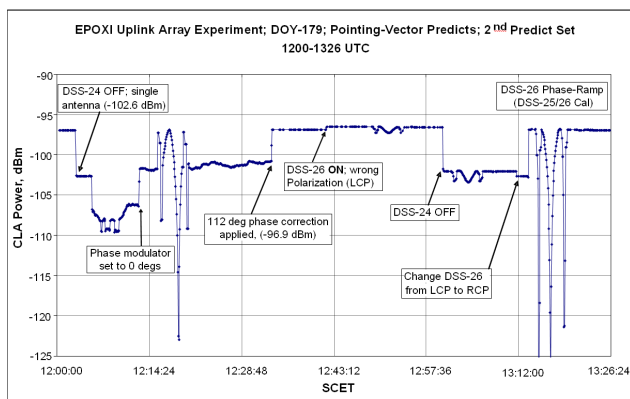


Figure 5b. Real-time CLA data, first part of second predict set.

Phase-ramping was initiated at 11:33 SCET via the digitally controlled phase modulator on the DSS-24 channel, in order to determine the optimum phase. This technique, termed “Nearby Spacecraft” calibration, was conducted on the DSS-24/25 baseline by ramping the DSS-24 phase from 0 to 2π radians at a rate of 2 degrees per second using the phase modulator assembly (PMA), and the downlinked spacecraft AGC power readings monitored in real-time at SPC-10. As can be seen in Fig. 5a, this resulted in an increase in measured array power from -102.7 dBm to -97 dBm, corresponding to a two-antenna array gain of 5.7 dB, close to the theoretically predicted 6 dB gain. Each phase-ramp consists of a preamble, which is a pattern of 0, 90, 180, 270 degrees applied for 10 seconds each, to mark the beginning of the ramp sequence, followed by a linear phase ramp of 2 degrees/second applied for 180 seconds, concluding with a repeat of the preamble pattern to help determine the end of the measurement sequence. The phase ramp itself always starts and ends at 0 degrees, to simplify the calibration process. The phase corresponding to maximum combined power is the desired calibration phase, which was determined to be 260 degrees for the first phase-ramp on the DSS-25/24 baseline. After applying the optimum phase, the combined power immediately jumped to -97 dBm at 11:45 SCET, verifying two-antenna power maximization.

Note that around 11:40 SCET, the combined power tends to fluctuate when the phase difference between the two antenna carriers is large, placing the combined signal on a steep part of the phase/power curve. On this part of the curve, the two-antenna array power changes rapidly with small phase variations, hence the array serves as a very sensitive instrument for measuring tropospheric fluctuations. As described in the insert in Fig. 5a, on the part of the power/phase curve corresponding to approximately 100 degrees of differential phase error, the combined power fluctuates near the single-antenna power level -103 dBm, likely due to differential tropospheric delay fluctuations on the order of 1 mm over the 258m baseline.

After verification of two-antenna combined power magnitude and stability, the first sequence of ten “arrayed” No-Op commands were transmitted to EPOXI by the two-antenna array, at approximately 11:50 SCET. Since the uplink subcarrier is 16 KHz, corresponding to a wavelength of 18.75 km, the maximum differential delay between any two antennas in the Apollo complex never exceeds 0.5 km/18.75 km = 0.027 wavelengths, hence can be neglected: this means that delay compensation is not required (0.5 km is the maximum extent of the array, along the DSS-24/26 baseline). Therefore, the modulation was distributed to all three antennas via an active three-way splitter/amplifier signal distribution assembly constructed especially for this purpose. The calibration curve for the EPOXI SDST with command “ON” is significantly different than with command “OFF” at high power levels (towards the left side of the curve), as can be seen in Fig. 5a. Unfortunately, the calibration curve was only available at a single temperature (25C), hence could not be interpolated to the much higher operating baseplate temperature of 42.5C. This is one of the reasons for the greater than the expected 5.8 dB drop in carrier power recorded by the CLA with modulation “ON”. Other contributing factors include uncalibrated test ports, and residual DC signal levels at the outputs of the signal distribution assembly which are converted directly to phase by the modulator, possibly spoiling the optimum phases relation between the two carriers during modulation.

The first predict set ended at 12:00:00 UTC, and approximately 3 minutes later at the spacecraft due to the one-way light-time. For the second tracking interval, the Pointing-vector based frequency predicts were selected, because these predicts were derived specifically for array applications and hence yielded consistent range and velocity estimates. The events of the second predict interval are depicted in Figs. 5b and c. After the pointing vector predicts were started, a phase-ramp calibration was initiated at 12:15 SCET, from which the optimum offset was determined to be 112 degrees, which indeed maximized the combined power at EPOXI at -96.9 dBm after application via the PMA. Next, the DSS-26 transmitter was turned on, and the signal reached EPOXI just before 12:43 SCET. The second phase-ramp on DSS-26 was initiated in order to calibrate the three-antenna array, however a total power variation of only about

1 dB was observed, instead of the expected 9.5 dB. Further tests led to the realization that the polarization of DSS-26 was accidentally set to LCP instead of RCP, causing large losses in received power from this station.

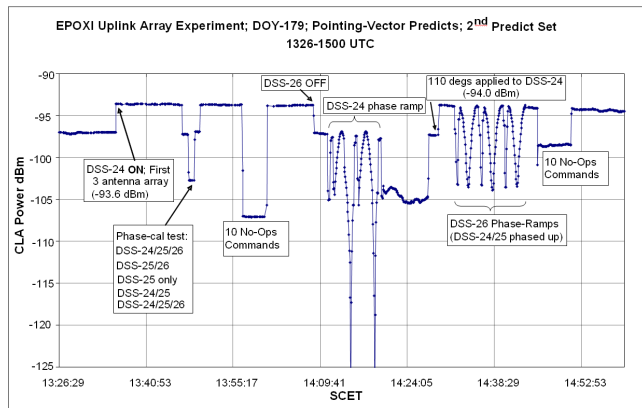


Figure 5c. Real-time CLA data, second part of second predict set.

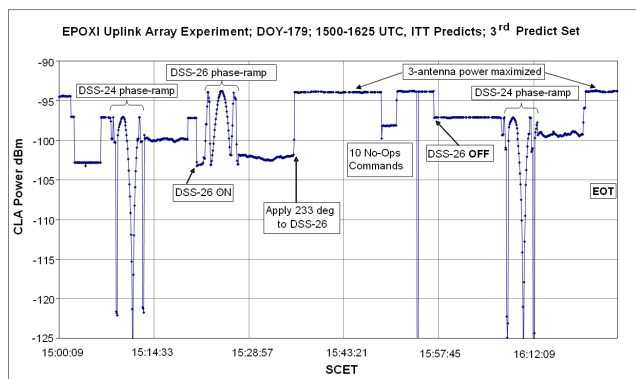


Figure 5d. Real-time CLA data, last part of experiment, third predict set.

To help determine the cause of the power drop, the DSS-24 transmitter was turned off at approximately 13:00 SCET (Fig. 5b), and a phase ramp applied to the DSS-26 PMA, which also produced only small power variations. After ruling out transmitter power anomalies and antenna pointing errors, it was postulated that DSS-26 may have been set up in the wrong polarization, LCP instead of RCP: this was indeed found to be correct.

After the DSS-26 polarization was reset to RCP, another two-antenna phase-ramp was initiated on the DSS-25/26 baseline, and the expected two-antenna response observed starting at 13:15 SCET. Following calibration along this baseline, the DSS-24 transmitter was turned back on, and the combined three-antenna power jumped to -93.6 dBm at about 13:36 SCET, close to the theoretically expected combined power of -93.3 dBm. Since the DSS-24/25 baseline was already calibrated and the frequency predicts maintained constant phase at the spacecraft, this two-antenna pairwise calibration successfully completed the three-antenna calibration process.

Successful three-antenna calibration via the pairwise method was followed by a phase symmetry test at 13:48 SC ET, where at first DSS-24 power was turned off, followed by DSS-26 to measure the single-antenna power of DSS-25, then the power of each was turned on in the opposite order. The slight asymmetry of the shoulders indicates somewhat better phase alignment along the DSS-24/25 baseline than along the DSS-25/26 baseline, which could account for some array gain loss, however it was not deemed significant. Another set of 10 No-Op commands were transmitted at 13:56 SCET, all of which were successfully received.

Starting at about 14:10 SCET, the DSS-24/25 baseline was recalibrated to reduce any small phase drifts since last calibration, in order to initiate the three-antenna calibration process. Here, a calibrated baseline is viewed as a single antenna, and the third antenna phase-ramped to maximize array power. Since a calibrated baseline consists of the sum of two carrier amplitudes, but phase-ramping of the third antenna can only cancel one of the amplitudes, the combined power varies between the three-antenna and single-antenna powers: this type of phase-ramp pattern can be seen in Fig. 5c, starting at about 14:30 SCET. Another set of 10 No-Op commands were transmitted at 14:45 SCET, before the end of the second frequency-predict set at 15:00 UTC.

For the third and final predict-interval, the ITT predicts were loaded in once again to obtain similar total data volumes for comparison (three hours of data for the Pointing-vector based predicts, two and a half hours total for the ITT predicts), and to facilitate more accurate comparison of data both at the beginning and the end of the long second predict-interval. In the third predict-interval, the three-antenna calibration was repeated, three-antenna stability data was collected, and one more set of No-Op commands transmitted successfully to EPOXI.

5. SUMMARY AND CONCLUSIONS

The first stable arraying of X-band carriers at interplanetary distances from up to three operational antennas has been demonstrated experimentally with the EPOXI spacecraft, on June 27, 2008. The experiment was carried out under realistic conditions at the Goldstone Deep-Space Communications Complex, using the 34 meter BWG antennas located at DSS-24, DSS-25 and DSS-26 of the Apollo complex. Doppler-compensated X-band carriers were transmitted to the spacecraft, and the concept of phase optimization to maximize received power demonstrated through the use of a novel phase-ramping algorithm suitable for operational use with future geo-stationary satellites, or lunar and “nearby spacecraft” transponders. Power maximization was achieved after each phase ramp, validating the predicted array gain, and fifty No-Op commands were transmitted to EPOXI at the maximum rate, all of which were received and acknowledged by the spacecraft. Differential phase remained stable during the entire experiment, proving that the newly developed array

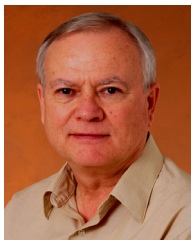
frequency predicts were sufficiently accurate to enable future operational uplink arraying.

Acknowledgements: The authors would like to thank Chris Jacobs (JPL) for providing the accurate, VLBI-derived position vectors for the Apollo cluster phase centers; Jonathan Walthers contributed to this effort by developing SPS predicts, and helped to analyze various experimental scenarios; Ryan Mukai deserves credit for significant contributions to the development of the LabView code used in the Phase Comparator and Control Assembly, and for simulating the Apollo cluster far-field array patterns of Fig. 4; we thank Jim Taylor for providing the original WBAGC and CLA SNR data records from the Telemetry Delivery Subsystem, shown in Figs. 10 and 11.

REFERENCES

1. V. Vilnrotter, Dennis Lee, "Uplink Array Experiment with the Mars Global Surveyor (MGS) Spacecraft," IPN-Progress Report 42-166, August 15, 2006.
2. V. Vilnrotter, D. Lee, R. Mukai, T. Cornish, P. Tsao, "Three-antenna Doppler-delay Imaging Of The Crater Tycho For Uplink Array_Calibration Applications," IPN Progress Report 42-169, May 15, 2007.
3. L. Paal, R. Mukai, V. Vilnrotter, T. Cornish, and D. Lee, "Ground System Phase Estimation Techniques for Uplink Array Applications," IPN Progress Report 42-167, November 15, 2006.
4. V. Vilnrotter, Mukai, Lee, "Uplink Array Calibration via Far-Field Power Maximization", IPN Progress Report 42-164, February 15, 2006.
5. V. Vilnrotter, D. Lee, R. Mukai, T. Cornish, P. Tsao, "Doppler-Delay Calibration of Uplink Arrays via Far-Field Moon-Bounce Power Maximization," Proceedings of the 11-th ISCOPS Conference, Beijing, May 15, 2007.

BIOGRAPHY



Victor Vilnrotter (M'79, SM'02) received his Ph.D. in electrical engineering and communications theory from the University of Southern California in 1978. He joined the Jet Propulsion Laboratory, Pasadena, Calif., in 1979, where he is a Principal Engineer in the Communications Systems Research section. His research interests include electronic compensation of large antennas with focal-plane arrays, adaptive combining algorithms for large antenna arrays, optical communications through atmospheric turbulence, the application of quantum communications to deep-space optical links, and the development of uplink

array calibration and tracking technologies. He has published extensively in conferences and refereed journals, and has received numerous NASA awards for technical innovations.



Dennis K. Lee (S'97 M'98) earned his B.S. from Case Western Reserve University in 1997 and his M.S. from Rensselaer Polytechnic Institute in 1998, both in Electrical Engineering. Since 1999, he has been a member of technical staff in the Digital Signal Processing Research group at the Jet Propulsion Laboratory. Currently, his research interests include bandwidth efficient modulations and high rate signal processing.



Timothy Cornish received a B.S. degree in Electrical Engineering from Illinois Institute of Technology in 1995. He has been employed in private industry in the high power transmitter field for over 15 years in positions ranging from Design Engineer to Engineering Department Manager. During that time he was responsible for system engineering and project management in the development of the 4 kW X-band High Power Amplifier recently in use in the Deep Space Network 34m Beam Waveguide Stations. Timothy joined the Jet Propulsion Laboratory in 2000 as a Transmitter Design Engineer in the Communications Ground Systems Section and is currently System Engineer for the Deep Space Network Uplink Subsystem. In his position as Transmitter Design Engineer he was responsible for the design of the 20 kW X-Band High Power Amplifier currently in use in the Deep Space Network 34m Beam Waveguide Stations.



Philip Tsao is a member of the Communications Networks Group at JPL. He received a BEE from Georgia Tech in 1999 and an MSEE from Caltech in 2001 where he pursued research in collective robotics. From 2001 and 2005 he was a Systems Engineer with Raytheon Space and Airborne Systems where he supported radar software and mixed signal circuit design efforts.



Leslie Paal is a member of the Systems

Engineering Group at JPL. He received a B.S. in Computer Science, and after years in the commercial world he joined JPL in 1985 where he is a Senior Engineer. At JPL he has been leading software, hardware and technology development programs as well as performing telecommunication engineer duties for operational mission. His interest is in ground station equipment automation, and unattended operations.



Vahraz Jamnejad is a principal scientist at the Jet Propulsion Laboratory, California Institute of Technology. He received his M.S. and Ph.D. in electrical engineering from the University of Illinois at Urbana, specializing in electromagnetics and antennas. At JPL, he has been engaged

in research and software and hardware development in various areas of spacecraft and ground base-station antenna technologies and satellite communication systems. In addition, he has been active in research in parallel computational Electromagnetics, optimization techniques and evolutionary programming for antenna system design and optimization. He is involved in the study of calibration techniques for the uplink arrays for the DSN, the development of Space Science Service (SRS) near/far field antenna models for the International Telecommunications Union, and studies of near field radiation effects of large antennas

